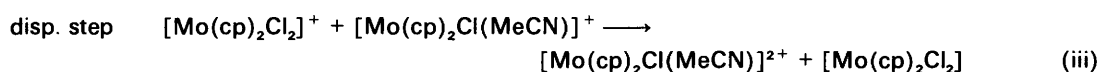
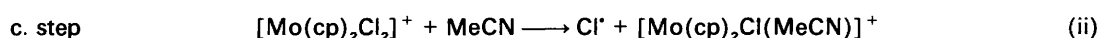
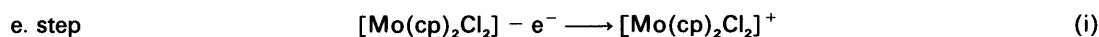


# Sono-electrochemistry: the Oxidation of Bis(cyclopentadienyl)molybdenum Dichloride

Richard G. Compton, John C. Eklund, Stephen D. Page and Thomas O. Rebbitt  
Physical Chemistry Laboratory, Oxford University, South Parks Road, Oxford OX1 3QZ, UK

The oxidation of  $[\text{Mo}(\text{cp})_2\text{Cl}_2]$  ( $\text{cp} = \eta\text{-C}_5\text{H}_5$ ) in acetonitrile solution at platinum electrodes has been studied. In the absence of ultrasound a simple one-electron oxidation with a half-wave potential of +0.5 V (vs. saturated calomel electrode) is observed together with a much smaller wave with a half-wave potential of +1.05 V. In the presence of ultrasound the first wave involves the passage of greater than one electron per molecule of electroactive species and the second wave disappears. The mechanism in equations (i)–(iii) is proposed to explain the observations, where the chemical (c.) (e. = electrochemical) and the disp. (disproportionation) steps are promoted by ultrasound.



Various workers have reported beneficial results from exposing electrochemical cells to the effects of ultrasound. Areas of application include electroplating,<sup>1,2</sup> the deposition of polymer films<sup>3,4</sup> and electrosynthesis.<sup>5,6</sup> However, whilst the value of ultrasound in these contexts is undisputed, prior work has been essentially of an applied or empirical nature and it is clearly desirable to develop an appreciation of the fundamental mechanisms by which ultrasound might modify electrode processes. Several possibilities are readily identified including (i) the enhancement of mass transport to and from the electrode surface resulting from cavitation in solution, (ii) the continuous activation of the electrode surface, (iii) the formation of ions, radicals and other high-energy intermediates during transient cavitation, and (iv) the ultrasonic mediation of chemical processes associated with heterogeneous electron-transfer steps.

The first three of these possibilities were addressed in previous papers.<sup>7–9</sup> The present paper seeks to illustrate the possible role of the ultrasonic mediation of *chemical* processes coupled to heterogeneous electron transfer. To this end we have employed the thermostatted cell shown in Fig. 1, the transport properties of which have been characterised previously,<sup>7</sup> and in which an ultrasonic horn is immersed in the solution of interest at a known distance above the working electrode under investigation. This arrangement was used to investigate the influence of ultrasound on the electrooxidation of bis(cyclopentadienyl)molybdenum dichloride in acetonitrile solution at both macro- and micro-electrodes. Under silent conditions this complex is known<sup>10,11</sup> to undergo a one-electron oxidation forming a cation which slowly substitutes according to the electrochemical step–chemical step–electrochemical step (e.c.e.) process shown in Scheme 1, where the second oxidation takes place at a more anodic potential than the first and the second step may proceed *via* the initial addition of MeCN. In the presence of ultrasound the electrode reaction changes so that an overall greater than one-electron process is observed at the potential of the first oxidation alone.

## Experimental

A VCX400 model sonic horn (Sonics and Materials, USA) was employed which had titanium-tipped probes (diameter 13 mm)

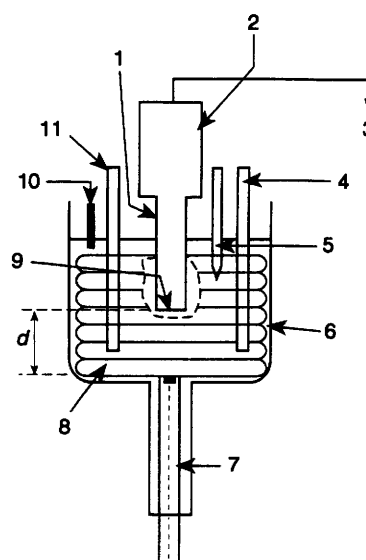
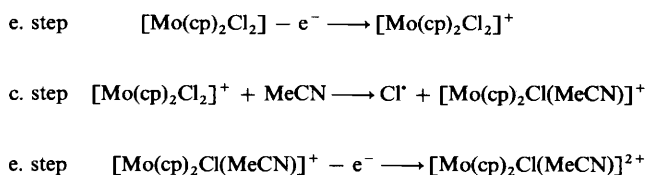


**Fig. 1** The sono-electrochemical cell used for the voltammetric studies: 1, sonic horn; 2, transducer; 3, to control unit of sonic horn; 4, graphite counter electrode; 5, argon inlet for degassing; 6, Pyrex reservoir; 7, platinum-disc macro- or micro-electrode; 8, copper cooling coil connected to the thermostatted water-bath; 9, titanium tip; 10, platinum resistance thermocouple; 11, SCE reference

which extended by 127 mm and operated at 20 kHz. Power levels up to and including  $55 \text{ W cm}^{-2}$  were used and calibrated calorimetrically according to the procedure of Mason *et al.*<sup>12</sup> Thermostating of the electrochemical cell was accomplished by means of a copper cooling coil inserted in the solution through which water was circulated from a constant-temperature bath. By limitation of the sonication time to less than 1 min this arrangement enabled the voltammetric measurements to be conducted at approximately constant temperature (to within  $2^\circ\text{C}$ ). A platinum-resistance thermometer (RS components, UK) was used to record the exact temperature (to within  $0.5^\circ\text{C}$ ) for each experimental run.



Scheme 1 cp =  $\eta\text{-C}_5\text{H}_5$

Platinum micro-disc electrodes were obtained from Bio-analytical Systems (West Lafayette, USA) and had radii between 2.5 and 60  $\mu\text{m}$  as measured electrochemically. Macroelectrodes of radii between 0.05 and 0.60 cm were mounted in an insulating Teflon sheath. All electrodes were carefully polished using diamond lapping compounds (Kemet, Kent, UK) of size decreasing to 0.25  $\mu\text{m}$ .

Voltammetric measurements were carried out using a Solatron 1286 electrochemical interface three-electrode potentiostat under computer control or an Oxford electrodes potentiostat. A carbon rod serviced as a counter electrode and a saturated calomel reference electrode (SCE) was located close to the working electrode surface as shown in Fig. 1.

The solvent used throughout was dried acetonitrile (Fisons, dried, distilled), and tetrabutylammonium perchlorate (Kodak, puris) served as the background electrolyte. Bis(cyclopentadienyl)molybdenum dichloride, tris(*p*-bromophenyl)amine and ferrocene (>98%, Aldrich) were used as received. Solutions were thoroughly purged of oxygen prior to electrolysis by outgassing with prepurified, dry argon.

Supporting theory was generated from programs written in FORTRAN 77 using double precision on a Sun IPC workstation.

## Results and Discussion

Initially experiments were conducted on the oxidation of bis(cyclopentadienyl)molybdenum dichloride in 0.1 mol dm<sup>-3</sup> NBu<sub>4</sub>ClO<sub>4</sub>-acetonitrile solution in the absence of ultrasound. Voltammetry (Fig. 2) showed the complex to undergo a reversible one-electron oxidation at a half-wave potential of +0.50 V (*vs.* SCE). A Tafel gradient of 60  $\pm$  5 mV per decade and a diffusion coefficient of  $(1.5 \pm 2) \times 10^{-5}$  cm<sup>2</sup> s<sup>-1</sup> were measured. At more anodic potentials a second, much smaller, oxidative wave was observed with a half-wave potential of 1.05 V *vs.* SCE and a Tafel gradient of 116  $\pm$  5 mV per decade indicating electrochemical irreversibility of the electrode process. All these observations are consistent with previous studies.<sup>10,11</sup> The second wave is the result of a one-electron oxidation of the product of decomposition of  $[\text{Mo}(\text{cp})_2\text{Cl}_2]^+$ , formed on the first wave, by the e.c.e. mechanism given in Scheme 1. The small size of the second wave reflects the slowness of the second step so that very little  $[\text{Mo}(\text{cp})_2\text{Cl}(\text{MeCN})]^+$  is formed on the voltammetric time-scale. The magnitude of the rate constant for this step under silent conditions was investigated by measuring the magnitude of the transport-limited current for the second wave as a function of electrode size using platinum micro-disc electrodes with radii in the range 2.5–60  $\mu\text{m}$ . The data were analysed by measuring the total effective number of electrons transferred in the first and second electrochemical (e.) steps of the e.c.e. mechanism ( $N_{\text{eff}}$ ) as a function of the disc radius ( $r_m$ ). The value of  $N_{\text{eff}}$  is related to the electrode radius for an e.c.e. process expression<sup>11,12</sup> (1)

$$N_{\text{eff}} = \frac{1}{\frac{4}{\pi} \left(\frac{D}{k}\right)^{\frac{1}{2}} \frac{1}{r_m} + 1} + 1 \quad (1)$$

where  $D$  is the diffusion coefficient of the electroactive species.

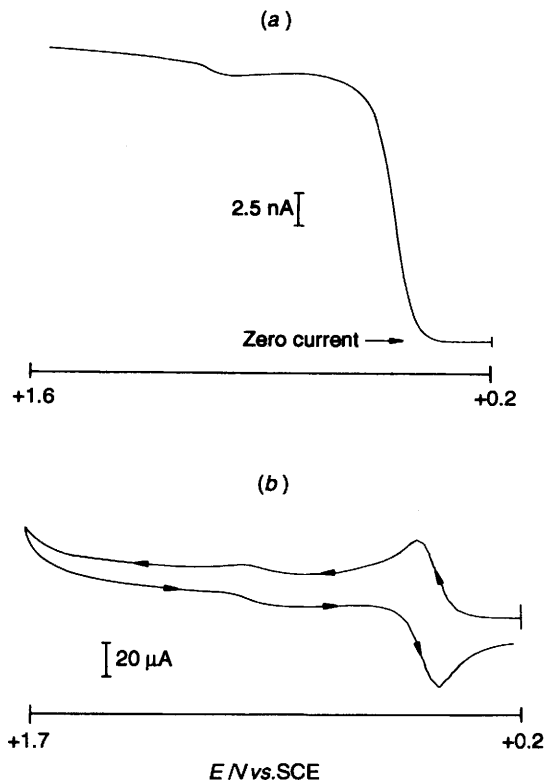


Fig. 2 Voltammetric waves for the oxidation of 1 mmol dm<sup>-3</sup>  $[\text{Mo}(\text{cp})_2\text{Cl}_2]$ –0.1 mol dm<sup>-3</sup> NBu<sub>4</sub>ClO<sub>4</sub>–acetonitrile measured using (a) a platinum microdisc electrode of radius 27  $\mu\text{m}$  and (b) a platinum-disc electrode of radius 0.30 cm

The experimental variation of  $N_{\text{eff}}$  with  $r_m$  was fitted by equation (1) using a least-squares analysis to find a best fit value of  $k$ ; Fig. 3 shows that a rate constant of  $k = 0.04$  s<sup>-1</sup> for the second step gives good agreement with the experimental data. This value is also in excellent agreement with that deduced *via* an independent method.<sup>13</sup>

Attention was then turned to the effect of ultrasound on the voltammetric response using the experimental arrangement shown in Fig. 1 with electrodes of radius between 2.5  $\mu\text{m}$  and 0.4 cm. Fig. 4 shows typical current *vs.* voltage curves recorded using ultrasound of power 55 W cm<sup>-2</sup> (20 kHz) directed at the electrode surface from a horn located 30 mm ( $d$ , Fig. 1) above it. Substantially larger currents were observed than in the absence of ultrasound and a clearly defined transport-limited current,  $I_{\text{lim}}$ , is attained at macro- as well as micro-electrodes, implying that a steady flux of the electroactive species towards the electrode from the bulk solution is promoted by the ultrasonically induced agitation of the solution. This effect has been discussed in detail elsewhere;<sup>7</sup> for the purposes of this work it suffices to note that mass transport in the system is quantitatively characterised by a thin diffusion layer immediately adjacent to the electrode of thickness,  $\delta_d$  [equation (2)],

$$I_{\text{lim}} = FAD[\text{Mo}(\text{cp})_2\text{Cl}_2]_{\text{bulk}}/\delta_d \quad (2)$$

where  $D$  is the diffusion coefficient of the electroactive molecule,  $F$  is the Faraday constant and  $A$  the electrode area. The average diffusion layer thickness was shown to depend on both the power of the ultrasound and on the electrode radius:<sup>7</sup>  $\delta_d$  was appreciably smaller for microelectrodes than for electrodes of conventional dimensions, although for both cases the diffusion layer thickness in the presence of ultrasound was significantly less than in the absence.

Measured values of  $I_{\text{lim}}$  were used to infer the effective average thickness of the diffusion layer in the presence of ultrasound (20

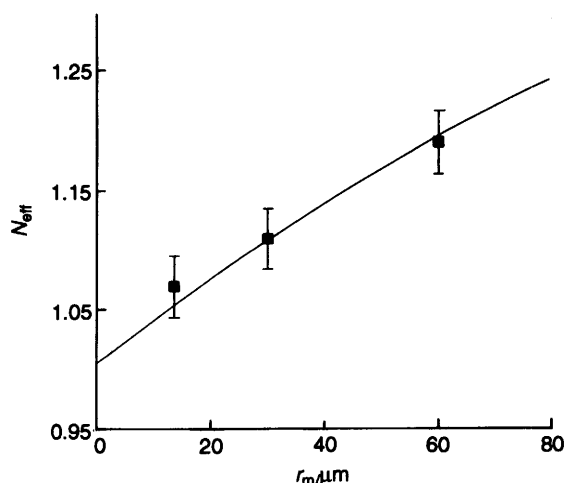


Fig. 3 The e.c.e. analysis of micro-disc results using equation (1). The solid line shows the variation of  $N_{\text{eff}}$  with micro-disc radius ( $r_m$ ) calculated using  $k = 0.04 \text{ s}^{-1}$  and the symbols ■ represent experimental data points

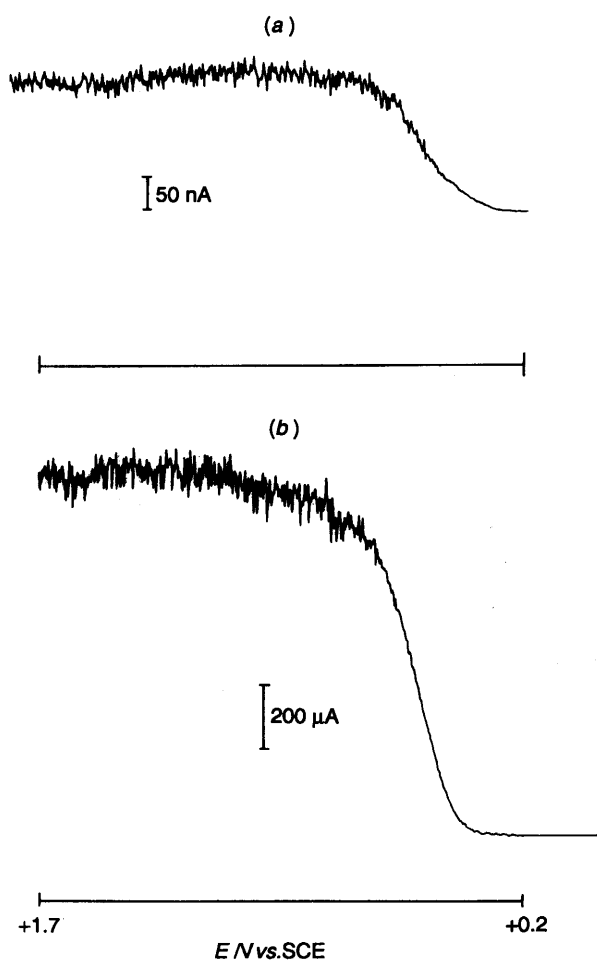


Fig. 4 Voltammetric waves for the oxidation of  $1.00 \text{ mmol dm}^{-3}$   $[\text{Mo}(\text{cp})_2\text{Cl}_2]$ – $0.1 \text{ mol dm}^{-3}$   $\text{NBu}_4\text{ClO}_4$ –acetonitrile measured with ultrasound ( $20 \text{ kHz}$ ,  $55 \text{ W cm}^{-2}$ ,  $d = 30 \text{ mm}$ ) directed at the electrode surface using (a) a platinum microdisc electrode of radius  $27 \mu\text{m}$  and (b) a platinum-disc electrode of radius  $0.30 \text{ cm}$

$\text{kHz}$ ,  $55 \text{ W cm}^{-2}$ ) for differently sized electrodes using the cell shown in Fig. 1 with  $d = 30 \text{ mm}$  to examine the simple one-electron oxidations of ferrocene and tris(*p*-bromophenyl)amine, both in acetonitrile– $0.1 \text{ mol dm}^{-3}$   $\text{NBu}_4\text{ClO}_4$  solution. In the

Table 1 Comparison of diffusion layer thicknesses for ultrasonically assisted oxidation of  $[\text{Fe}(\text{cp})_2]$  and tris(*p*-bromophenyl)amine

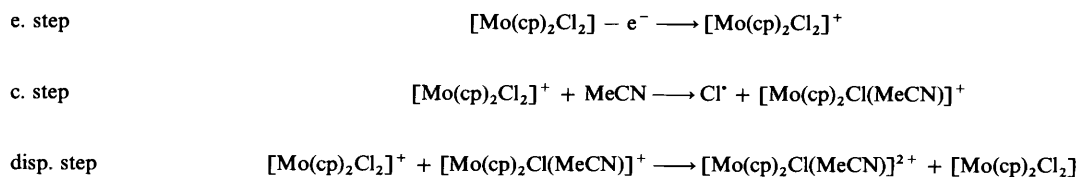
| Electrode radius  | $\delta_d/\mu\text{m}$     |   | Error/ $\mu\text{m}$ |
|-------------------|----------------------------|---|----------------------|
|                   | $[\text{Fe}(\text{cp})_2]$ | $\text{N}(\text{C}_6\text{H}_4\text{Br-}p)_3$ |                      |
| $27 \mu\text{m}$  | 3.1                        | 3.3   | $\pm 0.5$            |
| $60 \mu\text{m}$  | 4.3                        | 4.2   | $\pm 0.6$            |
| $0.10 \text{ cm}$ | 5.2                        | 5.0   | $\pm 0.7$            |
| $0.15 \text{ cm}$ | 5.6                        | 5.3   | $\pm 0.7$            |
| $0.30 \text{ cm}$ | 6.3                        | 6.3   | $\pm 0.7$            |

case of macroelectrodes equation (2) was used directly to obtain  $\delta_d$ , whereas for microelectrodes Hopscotch theory<sup>7</sup> was used to model the behaviour in the presence of ultrasound and so generated values of  $\delta_d$ . In this latter case  $\delta_d$  corresponds to the distance away from the microelectrode at which the concentrations attain their bulk values. The results, derived using literature values<sup>15,16</sup> for the diffusion coefficients of ferrocene ( $2.3 \times 10^{-5} \text{ cm}^2 \text{ s}^{-1}$ ) and tris(*p*-bromophenyl)amine ( $1.45 \times 10^{-5} \text{ cm}^2 \text{ s}^{-1}$ ), are summarised in Table 1. Good agreement between the two sets of experiments is apparent.

Next considered was the number of electrons passed under conditions of insonation by considering voltammograms such as shown in Fig. 4. In comparison with Fig. 2 it can be seen that large currents flow at potentials corresponding to the first oxidation wave ( $E_{\frac{1}{2}} = 0.50 \text{ V}$ ) but that the small wave at  $+1.05 \text{ V}$  is lost. Analysis of the transport-limited current of the  $+0.50 \text{ V}$  wave, in terms of equation (1), using the mean diffusion layer thicknesses given in Table 1 suggested that considerably more than one, but less than two, electron, was being passed. This is strongly suggestive of an e.c.e. or disp. (disproportionation) type process<sup>17</sup> in which the chemical step is accelerated in the presence of ultrasound. Accordingly the sonovoltammetry data were analysed in terms of the effective number of electrons transferred,  $N_{\text{eff}}$ , using the theory<sup>18</sup> for a mean uniform diffusion layer which predicts relationship (3) for an e.c.e.

$$N_{\text{eff}} = 2 - \frac{\tanh(\delta_d^2 k/D)^{\frac{1}{2}}}{(\delta_d^2 k/D)^{\frac{1}{2}}} \quad (3)$$

process, where  $k$  is the first-order rate constant describing the chemical step. Fig. 5 shows a working curve generated from equation (2) which permits interpretation of the experimental data. In particular experimental values of  $N_{\text{eff}}$  obtained at electrodes of different radius may be converted into corresponding values of the dimensionless quantity  $\delta_d^2 k/D$ . Then since  $\delta_d$  is known for each electrode and a value of  $D$  is available from the voltammetry conducted under silent conditions, it is possible to plot a graph of the experimentally determined quantity  $\delta_d^2 k/D$  against the known parameter  $\delta_d^2/D$ . In the case that the reaction so analysed is indeed of the e.c.e. type a straight line through the origin will indicate the correct choice of mechanism. Fig. 6 shows the data obtained for the bis(cyclopentadienyl)molybdenum dichloride system analysed according to this protocol. The line shown is that calculated theoretically for a rate constant of  $k = 300 \text{ s}^{-1}$  and the error bars deduced assuming an uncertainty of  $\pm 0.1$  in the determination of  $N_{\text{eff}}$ . It can be seen that reasonable agreement between theory and experiment is obtained suggesting that the process is indeed of the e.c.e. type. This mechanistic inference is further confirmed by Fig. 7 which shows the experimentally measured current plotted against that calculated using equation (2) for a rate constant of  $300 \text{ s}^{-1}$  for both macro- and microelectrodes. The units in the figure correspond to either  $\mu\text{A}$  or  $\text{nA}$  depending on the electrode size (see figure legend). This is done so as to show the comparison clearly for both electrode types in one figure as the currents for macro- and micro-electrodes differ



Scheme 2

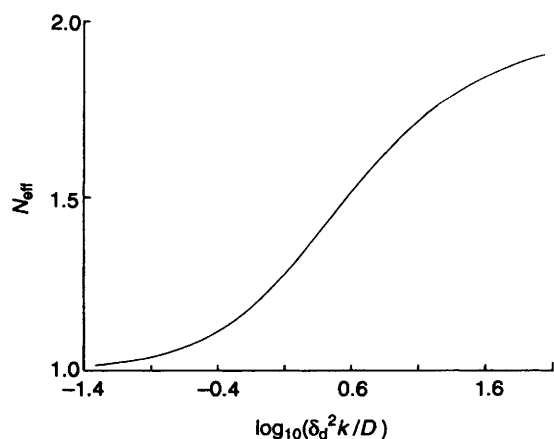


Fig. 5 A working curve for an e.c.e. process at an electrode with a mean diffusion layer thickness of  $\delta_d$

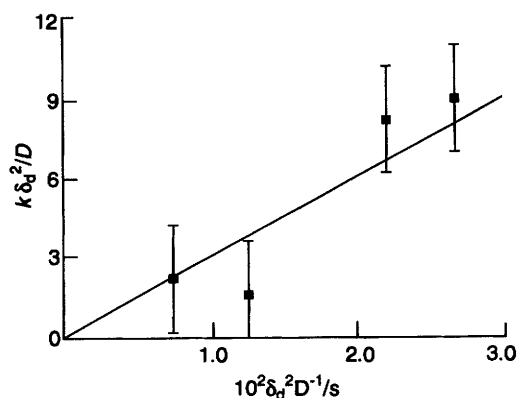


Fig. 6 Analysis of the transport-limiting current data obtained under conditions of insonation according to the protocol described in the text. The straight line drawn corresponds to a rate constant of  $300 \text{ s}^{-1}$

by three orders of magnitude. A good correlation is seen again confirming both the approach adopted and the mechanistic insight obtained.

We next speculate on the nature of the electrode process in the presence of ultrasound and note that in practice the difference between e.c.e. and disp. 1 (disproportionation, first order) mechanisms is usually too tiny to be experimentally resolvable<sup>19,20</sup> so that the analysis given above is consistent with either an e.c.e. or a disp. process. We suggest that the effect of ultrasound is to accelerate the second step resulting in very substantially greater quantities of  $[\text{Mo}(\text{cp})_2\text{Cl}(\text{MeCN})]^+$  being formed near the electrode surface. The absence of any further voltammetric features other than at the potential required for oxidation of the parent compound,  $[\text{Mo}(\text{cp})_2\text{Cl}_2]$  suggests that the electron transfer additional to the first step also arises from the discharge of  $[\text{Mo}(\text{cp})_2\text{Cl}_2]$ . This hints at a process in which there is a disproportionation between  $[\text{Mo}(\text{cp})_2\text{Cl}(\text{MeCN})]^+$  and  $[\text{Mo}(\text{cp})_2\text{Cl}_2]$  leading to regeneration of the parent species,  $[\text{Mo}(\text{cp})_2\text{Cl}_2]$ , so that the overall transformation under conditions of insonation is as in Scheme 2. In this scheme all the

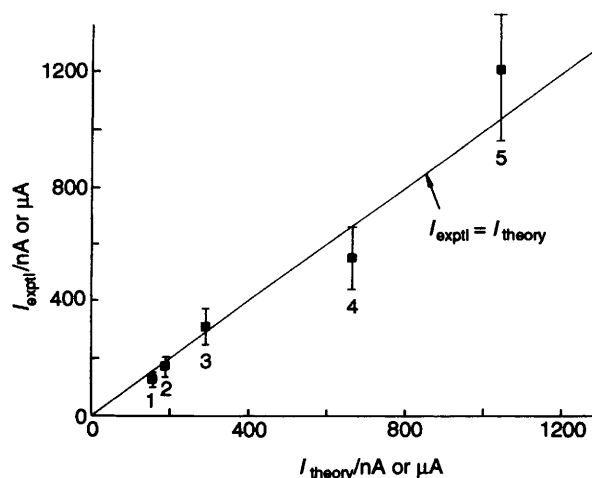


Fig. 7 Plot of the experimental limiting current measured under conditions of insonation against that calculated theoretically *via* equation (2) using a rate constant of  $300 \text{ s}^{-1}$ . The respective electrodes and current units are (1) 0.10 cm ( $\mu\text{A}$ ), (2) 27  $\mu\text{m}$  (nA), (3) 0.15 cm ( $\mu\text{A}$ ), (4) 60  $\mu\text{m}$  (nA) and (5) 0.30 cm ( $\mu\text{A}$ )

electron transfer derives from the oxidation of  $[\text{Mo}(\text{cp})_2\text{Cl}_2]$  so that only one voltammetric wave is seen with a half-wave potential of 0.50 V. Note first that the proposed disproportionation step may be thermodynamically downhill despite the formal potentials reported above since direct electrochemical oxidation of the cation,  $[\text{Mo}(\text{cp})_2\text{Cl}(\text{MeCN})]^+$ , to the corresponding dication is electrochemically *irreversible*. Thus the half-wave potential of 1.05 V may be very considerably more anodic than the true formal potential for the third step of Scheme 1. Secondly the absence of any voltammetric wave near +1.05 V in Fig. 4 corresponding to this step implies the removal of the species  $[\text{Mo}(\text{cp})_2\text{Cl}(\text{MeCN})]^+$  from the solution. This is consistent with the proposed mechanism if the disp. step is faster than the second step which would be the case for a disp. 1 process.

## Conclusion

The work reported describes a quantitative mechanistic assignment of an ultrasonically modified electrode reaction in which sono-sensitive chemistry is coupled to a heterogeneous electron-transfer event. Specifically, ultrasound is suggested to promote the substitution of the electrogenerated cation,  $[\text{Mo}(\text{cp})_2\text{Cl}_2]^+$ , and to induce a follow-up disproportionation reaction. Overall the effect is to facilitate the overall conversion of  $[\text{Mo}(\text{cp})_2\text{Cl}_2]$  into the two-electron oxidation product,  $[\text{Mo}(\text{cp})_2\text{Cl}(\text{MeCN})]^{2+}$ , at an applied voltage of +0.50 V as compared to the voltage of +1.05 V required under silent conditions to accomplish the same transformation with a much reduced efficiency as compared to that in the presence of ultrasound.

## Acknowledgements

We thank the EPSRC for a studentship (to J. C. E.) and the EC

for financial support (Contract No. CHRX CT94 0475) under the Human Capital and Mobility Scheme.

### References

- 1 R. Walker, *Chem. Br.*, 1990, **26**, 251.
- 2 B. Brown and J. E. Goodman, *High Intensity Ultrasonics*, Liffe Books, London, 1965.
- 3 U. Akbulut, L. Toppare and K. Yurrtas, *Polymer*, 1986, **27**, 803.
- 4 S. Oswana, M. Ito, K. Tanaka and J. Kuwano, *Synthetic Metals*, 1987, **18**, 145.
- 5 T. J. Mason, J. P. Lorimer and D. J. Walton, *Ultrasonics*, 1990, **28**, 333.
- 6 A. Chyla, J. P. Lorimer, G. Smith and D. J. Walton, *J. Chem. Soc., Chem. Commun.*, 1989, 603.
- 7 R. G. Compton, J. C. Eklund, S. D. Page, D. J. Walton and T. J. Mason, unpublished work.
- 8 R. G. Compton, J. C. Eklund, S. D. Page, G. H. W. Sanders and J. Booth, *J. Phys. Chem.*, 1994, **98**, 12410.
- 9 R. G. Compton, J. C. Eklund and S. D. Page, *J. Phys. Chem.*, in the press.
- 10 J. C. Kotz, W. Vining, W. Coco, R. Rosen, A. R. Dias and M. H. Garcia, *Organometallics*, 1983, **2**, 68.
- 11 M. Fleischmann, F. Lasserre and J. Robinson, *J. Electroanal. Chem. Interfacial Electrochem.*, 1984, **177**, 115.
- 12 J. Robinson, *Compr. Chem. Kin.*, 1989, **29**, 160.
- 13 R. G. Compton, J. Booth and J. C. Eklund, *J. Chem. Soc., Dalton Trans.*, 1994, 1711.
- 14 T. J. Mason and J. P. Lorimer, *Ultrasonics*, 1992, **30**, 140.
- 15 P. Sharp, *Electrochim. Acta*, 1983, **28**, 301.
- 16 A. C. Fisher, D.Phil. Thesis, Oxford University, 1991.
- 17 C. M. A. Brett and A. M. Oliveira Brett, *Electrochemistry. Principles, Methods and Applications*, Oxford Science Publications, OUP, Oxford, 1993, p. 123.
- 18 Y. V. Pleskov and V. Y. Filinovskii, *The Rotating Disc Electrode*, Plenum, New York, 1976, p. 243.
- 19 C. Amatore, M. Gareil and J. M. Savéant, *J. Electroanal. Chem. Interfacial Electrochem.*, 1983, **147**, 1.
- 20 C. Amatore and J. M. Savéant, *J. Electroanal. Chem. Interfacial Electrochem.*, 1977, **85**, 27.

Received 30th August 1994; Paper 4/05254D